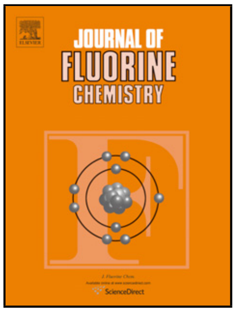

Title: Crystal structures of phases observed in $[H_3O]^+/M^{2+}/[SbF_6]^-$ system (M = Mg, Cr, Mn, Fe, Co, Ni, Cu, Zn, Pd, Cd)

Author: Zoran Mazej Evgeny Goreshnik

PII: S0022-1139(16)30415-8
DOI: http://dx.doi.org/doi:10.1016/j.jfluchem.2016.11.021
Reference: FLUOR 8908

To appear in: *FLUOR*

Received date: 26-10-2016
Revised date: 24-11-2016
Accepted date: 28-11-2016

Please cite this article as: Zoran Mazej, Evgeny Goreshnik, Crystal structures of phases observed in [H3O]+/M2+/[SbF6]− system (M=Mg, Cr, Mn, Fe, Co, Ni, Cu, Zn, Pd, Cd), Journal of Fluorine Chemistry http://dx.doi.org/10.1016/j.jfluchem.2016.11.021

Crystal structures of phases observed in $[H_3O]^+$/ M^{2+} / $[SbF_6]^-$ system (M = Mg, Cr, Mn, Fe, Co, Ni, Cu, Zn, Pd, Cd)

Zoran Mazej*, Evgeny Goreshnik

Jožef Stefan Institute, Jamova 39, SI-1000 Ljubljana, Slovenia, zoran.mazej@ijs.si

Phone: (+386) 1 477 3301

Graphical abstract

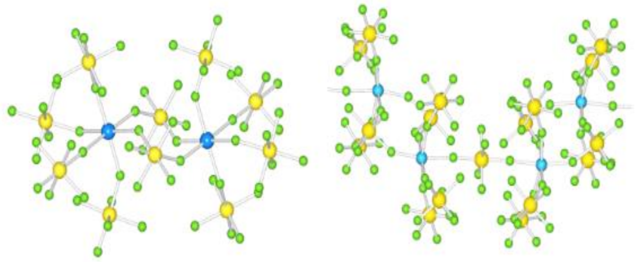

Highlights

- $H_3OM(SbF_6)_3$ (M = Mg, Co, Ni Fe, Cu and Zn) compounds crystallize isotypically.
- Slow crystallizations of H_3OSbF_6 / $M(SbF_6)_2$ (M = Mn, Pd, Cd) mixtures result in a new type of compounds, i.e. $(H_3O)_3M(SbF_6)_5$.
- Crystal structure of each $(H_3O)_3M(SbF_6)_5$ (M = Mn, Pd, Cd) represents a unique case.
- Discrete $[Cr^{IV}(SbF_6)_6]^{2-}$ units are present in $(H_3O)_3[Cr^{IV}(SbF_6)_6](Sb_2F_{11})\cdot HF$.

Abstract

The reactions between the MO (M = Be, Mg, Ca, Sr, Ti, V, Nb, Mn, Ni, Cu, Pd, Zn, Hg, Sn, Pb) and SbF_5 in liquid aHF were investigated. Reactions with the MO (M = Mg, Ni, Cu and Zn) yielded $H_3OM(SbF_6)_3$ compounds. Both BeO and PdO didn't show any sign of reactivity meanwhile MO (M = V, Nb, Ti) gave products with M in oxidation state higher than two. The rest of the MO (M = Ca, Sr, Mn, Hg, Sn, Pb) formed mixtures of $M(SbF_6)_2$, H_3OSbF_6 and/or $H_3OSb_2F_{11}$. Reactions between H_3OSbF_6 and $M(SbF_6)_2$ (M = Fe, Co, Ni) also gave $H_3OM(SbF_6)_3$ compounds, meanwhile similar attempts with H_3OSbF_6 and $M(SbF_6)_2$ (M = Ca, Mn, Pd, Ag, Cd, Sn) to prepare $[H_3O]^+/M^{2+}/[SbF_6]^-$ salts failled. However, slow crystallizations of H_3OSbF_6 and $M(SbF_6)_2$ (M = Mn, Pd, Cd) mixtures resulted in the single crystal growth of new $(H_3O)_3M(SbF_6)_5$ phases which crystal structures are not isotypic. Similar procedure with H_3OSbF_6 / $Cr(SbF_6)_2$ mixture resulted in few light orange crystals of $(H_3O)_3[Cr^{IV}(SbF_6)_6](Sb_2F_{11})\cdot HF$. Its crystal structure determination showed the presence of discrete $[Cr^{IV}(SbF_6)_6]^{2-}$ units where each of Cr atoms is found in a homoleptic coordination of six SbF_6 groups.

Keywords: Oxonium salt; Hexafluoridoantimonate; Superacid; Crystal structure, Oxide.

1. Introduction

Metal oxides MO (M = Mn, Zn, Cu) react with AsF_5 in anhydrous hydrogen fluoride (aHF) yielding oxonium salts $H_3OM(AsF_6)_3$ (Mn, Zn) or $H_3OMF(AsF_6)_2$ (M = Cu), respectively.[1] Few single crystalls of $(H_3O)_2Hg_2F(AsF_6)_5$ were grown from solution of HgO in aHF acidified with large excess of AsF_5.[1] The compounds, $H_3OM(AsF_6)_3$, can be also prepared by a reaction between H_3OAsF_6 and $M(AsF_6)_2$ (M = Mn, Co, Ni, Fe, Zn), meanwhile similar reaction between H_3OAsF_6 and CrF_2 in aHF acidified with AsF_5 gives only a mixture of H_3OAsF_6 and $CrFAsF_6$.[1,2,3] In the CdO/SbF_5/aHF system, the crystal structures of $H_3OCd(SbF_6)(Sb_2F_{11})_2$, $(H_3O)_2Cd(SbF_6)_3(Sb_2F_{11})$, $(H_3O)_2Cd_2F(SbF_6)_5$ and $(H_3O)[Cd(HF)]_4(SbF_6)_9$ were determined.[4] Attempts to prepare $[H_3O]^+/M^{2+}/[AsF_6]^-$ compounds, using TiO, VO, NbO, PdO, CdO, HgO, SnO and PbO, were unsuccessful.[1]

Since $[SbF_6]^-$ anion is only slightly larger than $[AsF_6]^-$ anion, is therefore not surprising that crystal structures of many corresponding $[AsF_6]^-$ and $[SbF_6]^-$ salts are isotypic. In the present study the reactions between MO (M = Be, Mg, Ca, Sr, Ti, V, Nb, Mn, Ni, Cu, Pd, Zn, Hg, Sn, Pb) and SbF_5 in liquid aHF were conducted to find out whether the same type of compounds as in in the $[H_3O]^+/M^{2+}/[AsF_6]^-$ system would be obtained, or whether the larger size of $[SbF_6]^-$ would lead to the formation of new products. Additionally, some reactions between H_3OSbF_6 and $M(SbF_6)_2$ (M = Ca, Cr, Mn, Fe, Co, Ni, Pd, Ag, Cd, Sn) in aHF were investigated.

2. Results and Discussion

2.1. Syntheses

There were no reactions between MO (M = Be, Pd) and SbF_5 in aHF (**Table 2**). Reactions between MO (M = V, Ti, Nb) and SbF_5 in aHF resulted in products with M in oxidation state higher than two. These findings are in agreement with the results of reactions between the MO (M = V, Ti, Nb) and AsF_5 in aHF.[1] The MO (M = V, Ti, Nb) don't react with pure liquid aHF. The $[SbF_6]^–$, the dominant species in diluted SbF_5/aHF solutions - as used in this work, is a much weaker oxidant than molecular SbF_5. Therefore, the higher oxidation state M^{n+} (n = 3, 4 and/or 5) in isolated products are a consequence of disproportionation of low-oxidation-state M^{2+} cations.[5] For example, the $[Ti(HF)_6]^{2+}$ is stable only in a narrow "window" of acidity, i.e., only in aHF solutions containing SbF_5 at concentrations between 2 and 3 M.[5] During reactions between MO and SbF_5 in liquid aHF oxygen atoms are protonated yielding $[H_3O]^+$ cations meanwhile initial formation of solvated low-oxidation-state $[M(HF)_n]^{2+}$ cations is followed by disproportionation to metallic form and higher fluorides. The finely divided metals would redissolve to give M^{n+}.

Reactions between the MO (M = Ca, Sr, Mn, Hg, Sn, Pb) and SbF_5 in aHF yielded mixtures of H_3OSbF_6/$H_3OSb_2F_{11}$ and $M(SbF_6)_2$. With exception of Mn, the same trend was observed in the AsF_5 system. [1]

Reactions between metal oxides MO (M = Mg, Ni, Cu, Zn) and SbF_5 in aHF yielded oxonium salts $H_3OM(SbF_6)_3$. Same type of products was obtained by reacting of H_3OSbF_6 with $M(SbF_6)_2$ (M = Fe, Co, Ni) in aHF.

After attempted reactions between between H_3OSbF_6 and $M(SbF_6)_2$ (M = Ca, Mn, Sn) only starting materials were recovered (**Table 3**). Slow crystallizations from H_3OSbF_6 and $M(SbF_6)_2$ (M = Mn, Pd, Cd) mixtures resulted in a new type of compounds, i.e. $(H_3O)_3M(SbF_6)_5$. Single crystal structure determinations revealed that all three compounds are not isotypic with each other. In the case of Mn the isolated $[H_3O]^+$/M^{2+}/$[AsF_6]^-$ salt corresponds to $H_3OMn(AsF_6)_3$ [3] meanwhile no such product was observed for larger $[SbF_6]^-$ anion. The prolonged crystal growth from H_3OSbF_6 and $Cr(SbF_6)_2$ crystallization mixture gave few light orange single crystals of $(H_3O)_3[Cr^{IV}(SbF_6)_6](Sb_2F_{11})\cdot HF$. The same type of crystals was obtained after crystallization from XeF_5SbF_6 and $Cr(SbF_6)_2$ mixture in aHF.[6] There the presence of Cr(IV) could be explained by oxidation of Cr(II) with $[XeF_5]^+$. In the H_3OSbF_6/$Cr(SbF_6)_2$/aHF system the low oxidation state Cr^{2+} cations could reduce protons from $[H_3O]^+$, releasing water which is a strong base in aHF and it is again protonated by the solvent, i.e. superacid HF.[7] This would only explain the oxidation of Cr^{2+} to Cr^{3+}. During long-lasting crystallizations there is a possibility of diffusion of water vapor through the walls of the reaction vessel, made of fluorocarbon polymers.[8] Superacids are good media to stabilize low oxidation state cations, but lowered acidities can lead to disproportionation.[5] It might be possible that the presence of $[H_3O]^+$ itself could be sufficient to initiate disproportionation of Cr(II) yielding Cr(IV) compound.

2.2. Crystal structures of $H_3OM(SbF_6)_3$ (A = Mg, Fe, Co, Ni, Cu, Zn) and $(H_3O)_3M(SbF_6)_5$ (M = Mn, Pd, Cd)

Compounds of the type of $H_3OM(SbF_6)_3$ (M = Mg, Fe, Co, Ni, Cu, Zn) are isotypic with the known $H_3OM(AsF_6)_3$ (Fe, Co, Ni, Zn, Mn) compounds.[1,2,3,9] The sizes of M^{2+} crystal radii are very similar (the M^{2+} sizes for the coordination number six increase in the order Ni < Mg

< Cu < Zn < Co < Fe < Mn [10]). Since there haven't been any indications about existence of $H_3OMn(SbF_6)_3$, it seems that the combination of larger Mn^{2+} and $[SbF_6]^–$ ions is on the border of stability of the main feature of the crystal structures of isotypic $H_3OM(XF_6)_3$ (M = divalent metal, X = As, Sb) compounds, i.e. three-dimensional $[M(XF_6)_3]^–$ framework composed of M^{2+} cations interconnected by XF_6 octahedra, forming cavities within which $[H_3O]^+$ cations are located (**Fig. 1**). Therefore, Mn^{2+} prefers to form $(H_3O)_3Mn(SbF_6)_5$ instead of $H_3OMn(SbF_6)_3$. The influence of larger Mn^{2+} is also evident in the case of $XeF_5M(SbF_6)_3$ (M = Ni, Mg, Cu, Zn, Co, Mn, Pd) compounds. Their crystal structures consist of similar three-dimensional $[M(XF_6)_3]^–$ framework as in $H_3OM(XF_6)$ (M = divalent metal, X = As, Sb) compounds (**Fig. 1**), although slightly modified for larger Mn and Pd.[6] Since the sizes of the Pd^{2+} (1.00 Å for C.N. = 6) and Cd^{2+} (0.95 Å for C.N. = 6) [10] are close to that of Mn^{2+} (0.97 Å) [10] is not unexpected that they also form different types of compounds, i.e. $(H_3O)_3M(SbF_6)_5$ (M = Cd, Pd), as smaller M^{2+} cations (M = Mg, Fe, Co, Ni, Cu, Zn).

Summary of the refinement results and other crystallographic information for $H_3OMg(AsF_6)_3$, $(H_3O)_3M(SbF_6)_5$ (M = Mn, Pd) and $(H_3O)_3[Cr^{IV}(SbF_6)_6](Sb_2F_{11})\cdot HF$ are provided in Table 1.

The crystal structure of $(H_3O)_3Mn(SbF_6)_5$ consists of infinite zig-zag $([Mn_2(SbF_6)_9]^{5-})_n$ columns, i.e. –(trans-η^2-SbF_6)–[Mn(η^1-SbF_6)$_3$]–(cis-η^2-SbF_6)$_2$–[Mn(η^1-SbF_6)$_3$]– (**Fig. 2**), oriented parallel to each other along *b*-axis (**Fig. S1**). Free $[SbF_6]^-$ (Sb6) anions, and $[H_3O]^+$ cations (which provide additional positive charge) are located between the columns.

Within each $([Mn_2(SbF_6)_9]^{5-})_n$ column two adjacent Mn atoms are bridged by two SbF_6 (Sb2) units with the bridging F atoms in cis-position. Each of Mn is additionally linked to one neighbouring Mn atom by one SbF_6 (Sb1) unit with the bridging F atoms in trans position. The coordination around each Mn is completed with three terminal SbF_6 (Sb3, Sb4, Sb5) groups. On such a way, manganese is octahedrally coordinated with six F atoms with Mn–F distances (2.087(3) - 2.146(3) Å) that correlate well with the values of Mn–F bond lengths (2.118(4) - 2.133(4) Å) determined in $Mn(SbF_6)_2$.[11] The Sb–F_b bonds (F_b = bridging fluorine atom; 1.907(3) - 1.925(3) Å) are elongated relative to the Sb–F_t bonds (F_t = terminal fluorine atom; 1.835(3) - 1.881(3) Å). The corresponding Sb–F_b and Sb–F_t bonds in $Mn(SbF_6)_2$ are in the range 1.918(4) - 1.941(4) Ǻ and 1.832(4) - 1.856(4) Ǻ, respectively.[11]

Although Pd compound has similar formula, i.e. $(H_3O)_3Pd(SbF_6)_5$, it is not isotypic with Mn compound. It crystallizes in two crystal modifications at low (α-phase, 200 K) and ambient (β-phase, 293 K) temperatures. α-$(H_3O)_3Pd(SbF_6)_5$ crystallizes in monoclinic space group, meanwhile β-phase is triclinic (**Table 1**). Beside more dense packing in the α-phase, with a packing index of 75.6% whereas respective value for the β-phase is 73.5%, there are no significant differences between both phases. Therefore, only description of crystal structure of the high-temperature phase is given.

The mean structural feature of $(H_3O)_3Pd(SbF_6)_5$ represents $[Pd(\eta^1\text{-}SbF_6)_4]$–(cis-$\eta^2$-$SbF_6)_2$–$[Pd(\eta^1\text{-}SbF_6)_4]$ moiety consisted of two Pd atoms bridged by two SbF_6 (Sb2) units (**Fig. 3**). The coordination of each Pd is completed by four terminal SbF_6 (Sb1, Sb3, Sb4, Sb5) groups. The $[H_3O]^+$ cations are located between the anionic moieties (**Fig. S2**). The Pd–F bonds range from 2.163(2) Å to 2.203(2) Å (β-phase) and from 2.150(5) to 2.209(5) Å (α-phase). The Pd–F bond lengths in $Pd(AsF_6)_2$ are equal to 2.183(5) - 2.190(5) Å.[12] The Sb–F bonds are of similar length as in $(H_3O)_3Mn(SbF_6)_5$ (α-phase: Sb–F_b = 1.913(5) - 1.941(5) Å, Sb–F_t = 1.832(6) - 1.878(5) Å; β-phase: Sb–F_b = 1.908(2) - 1.926(2) Å, Sb–F_t = 1.820(3) - 1.877(3) Å).

The numerous repeated attempts to obtain the good-quality X-ray diffraction data of $(H_3O)_3Cd(SbF_6)_5$ were unsuccessful. The structure refinement did not lead to the satisfactory results. Therefore, the given structure is to be understood as merely modelling connectivity where is clearly visible that it represents the third structure type of $(H_3O)_3M(SbF_6)_5$ (M = Mn, Pd, Cd) compounds. In contrast to $(H_3O)_3M(SbF_6)_5$ (M = Mn, Pd) where crystal structure of the former consists of $([Mn_2(SbF_6)_9]^{5-})_n$ columns, "free" $[SbF_6]^-$ anions and $[H_3O]^+$ cations, and crystal structure of the latter of $[Pd(SbF_6)_4]$–$(SbF_6)_2$–$[Pd(SbF_6)_4]$ moieties and $[H_3O]^+$ cations, the crystal structure of $(H_3O)_3Cd(SbF_6)_5$ is a three-dimensional framework formed of Cd atoms linked through SbF_6 groups forming cavities within which "free" $[SbF_6]^-$ anions and $[H_3O]^+$ cations are located (**Fig. S3**).

It's well known that oxygen and fluorine atoms are sometimes technically difficult to distinguish by X-ray diffraction. In the crystal structure of yellow-orange $(H_3O)_3[Cr^{IV}(SbF_6)_6](Sb_2F_{11})\cdot HF$ the positions of hydrogen atoms could not be unambiguously determined. Therefore, grown crystals could hypothetically also correspond to the $(H_3O)_2[Cr^{V}(SbF_6)_6](Sb_2F_{11})\cdot 2HF$ if we assume that one of the $[H_3O]^+$ cations is in reality HF. Option with Cr^{III}, i.e. $(H_3O)_4[Cr^{III}(SbF_6)_6](Sb_2F_{11})$, has been excluded on the basis that Cr(III) fluoride compounds are green. The possibility that instead of some of HF molecules or H_3O groups we have only free fluoride anions ($F^{–}$) is also unlikely. Therefore only two possibilities were taken into account, i.e., $(H_3O)_3[Cr^{IV}(SbF_6)_6](Sb_2F_{11})\cdot HF$ and $(H_3O)_3[Cr^{V}(SbF_6)_6](Sb_2F_{11})\cdot 2HF$. Chromium compounds with a Cr(V) in a fluoride environment are red to deep red, meanwhile chromium compounds, with Cr(IV) coordinated to fluoride ligands, are yellow, orange or brick red. On the basis of that we assume that the formulation $(H_3O)_3[Cr^{IV}(SbF_6)_6](Sb_2F_{11})\cdot HF$ is correct. Additionally, average $Cr–F_{av}$ bond distance (1.888 Å) in $(H_3O)_3[Cr^{IV}(SbF_6)_6](Sb_2F_{11})\cdot HF$ is closer to $Cr^{IV}–F_{av}$ bond lengths in CrF_4 (1.836 Å),[13] $RbCrF_5$ (1.824 Å),[14] $CsCrF_5$ (1.810 Å),[14] $K_2CrF_6\cdot 2HF$ (1.820 Å) [14] than to $Cr^{V}–F_{av}$ bond lengths determined in Cr(V) fluorides ($NaCrF_6$ (1.740 Å) [14], $KCrF_6$: 1.750 Å [14]; $RbCrF_5$: 1.7582 Å [14]).

The crystal structure of $(H_3O)_3[Cr^{IV}(SbF_6)_6](Sb_2F_{11})\cdot HF$ consists of $[Cr(SbF_6)_6]^{2–}$ groups, $[Sb_2F_{11}]^{–}$ anions, non-coordinated HF molecules and $[H_3O]^{+}$ cations. There are two crystallographically independent Sb_2F_{11} units. First Sb_2F_{11} unit (Sb7/Sb8) has completely ordered F ligands, meanwhile part of the second Sb_2F_{11} group (Sb9/Sb10) is disordered. The Sb10 atom was split over two position, i.e., Sb10 and Sb11. Despite the rather large thermal ellipsoids of some fluorine atoms connected to the Sb(10/11), all attempts to split their positions (with exception of F94) to obtain a reasonable model of the disordering were unsuccessful.

The most interesting feature in the crystal structure of $(H_3O)_3[Cr^{IV}(SbF_6)_6](Sb_2F_{11})\cdot HF$ is the presence of discrete $[Cr(SbF_6)_6]^{2–}$ groups where each is Cr(IV) is found in a homoleptic coordination of six SbF_6 groups (**Fig. 4**). Such moieties haven't been observed before.

2.3. Raman spectra of $H_3OM(SbF_6)_3$ (A = Mg, Fe, Co, Ni, Cu, Zn) compounds

Raman spectra of $H_3OM(SbF_6)_3$ (A = Mg, Fe, Co, Ni, Cu, Zn) are shown in **Fig. 5** and **Fig. S4** (Supplementary Material). Since they all show similar features only Raman spectrum of Mg compound is discussed.

The bands at 671, 596, and 305/292/275 cm^{-1} are assigned to the v_1 (A_{1g} symmetry) and v_2 (E_g symmetry) Sb–F stretching normal modes and the v_5 (T_{2g} symmetry) bending normal modes, respectively, of $[SbF_6]^{–}$ anion. Bands in the region 500–560 cm^{-1} are typical for species where one fluorine bridges two different atoms, and can be readily assigned to *M*–F–Sb stretching modes. The rest of the bands (213 and 119 cm^{-1}) belongs to lattice vibrations. The similarity of Raman spectra (**Fig. 5** and **Fig. S4**) agrees with X-ray single crystal (Mg) and X-ray powder diffraction results (**Table S1**) which show that all $H_3OM(SbF_6)_3$ (A = Mg, Fe, Co, Ni, Cu, Zn) compounds are isotypic.

3. Conclusions

The $H_3OM(SbF_6)_3$ (Mg, Fe, Co, Ni, Cu Zn) compounds can be prepared from the corresponding oxides (MO; M = Mg, Ni, Cu, Zn) and/or by reactions between H_3OSbF_6 and $M(SbF_6)_2$ (M = Fe, Co). They crystallize isotypically with $H_3OM(AsF_6)_3$ (M = Mn, Co, Ni, Fe, Zn) compounds.[1,2,3]

Reactions between H_3OSbF_6 and $M(SbF_6)_2$ (M = Mn, Pd) were unsuccessful meanwhile slow crystallizations of H_3OSbF_6 and $M(SbF_6)_2$ (M = Mn, Pd, Cd) mixtures resulted in a new type of compounds, i.e., $(H_3O)_3M(SbF_6)_5$, where each crystal structure represents a unique case. It seems that $(H_3O)_3M(SbF_6)_5$ is the thermodynamically more stable product, while H_3OSbF_6 and $M(SbF_6)_2$ are favoured kinetically.

The use of H_3OSbF_6 / $Cr(SbF_6)_2$ mixture led to the growth of few light yellow-orange crystals of $(H_3O)_3[Cr^{IV}(SbF_6)_6](Sb_2F_{11})\cdot HF$ which were found on the surface of green undissolved material. The crystal structure determination has shown the presence of discrete $[Cr^{IV}(SbF_6)_6]^{2-}$ units where each Cr atom is found in a homoleptic coordination of six SbF_6 units.

The attempts to synthesize $[H_3O]^+/M^{2+}/[SbF_6]^-$ salts with M^{2+} = Be, Ca, Sr, Ti, V, Nb, Ag, Hg, Sn, Pb) failled.

4. Experimental

4.1. Apparatus and Reagents

All the manipulations were carried out under anhydrous conditions. The volatile compounds, such as aHF, SbF_5 and F_2, were handled on a vacuum line constructed from nickel-Teflon and the non-volatile materials were handled in a dry box (M. Braun) in an argon atmosphere (<0.5 ppm H_2O). Reactions were carried out in FEP (tetrafluoroethylene-hexafluoropropylene; Polytetra GmbH, Germany) reaction vessels (height 250–300 mm with inner diameter 15.5 mm and outer diameter 18.75 mm) equipped with PTFE valves [15] and PTFE coated stirring bars. Before use all reaction vessels were passivated with elemental fluorine (Solvay Fluor and Derivate GmbH, Germany). BeO (Schuchardt Munchen), MgO (Merck, >97 %), TiO (Alfa Aesar, 99.5%), VO (Alfa Aesar, 99.5 %), MnO (Alfa Aesar, 99.99 %), NiO (Ventron, 99%), CuO (Alfa Aesar, 99.9 %), PdO (Alfa Products, 99.9 %), ZnO

(Sigma Aldrich, 99.99 %), NbO (Alfa Aesar), CdO (Sigma Aldrich, 99.5 %), HgO (Alfa Aesar, 99 %), SnO (Alfa Aesar, 99.9 %), PbO (Johnson Matthey GmbH, 99.99%), CaF_2 (Merck), CrF_2 (ABCR, 99 %), MnF_2 (Alfa Aesar, 99 %), CoF_2 (Johnson Matthey GmbH, 99 %), NiF_2 (Alfa Products, 99.9%), SnF_2 (Aldrich, 99 %) were used as supplied. CaO (Kemika Zagreb) was treated for 5 h at 1100 ^{o}C in air atmosphere, SrO was prepared from $SrCO_3$ (Riedel de Haen, pure) at 1000 ^{o}C in air atmosphere, CdF_2 was prepared by pressure fluorination of $CdCl_2{\cdot}H_2O$ with elemental fluorine in liquid aHF in FEP reaction vessel, FeF_2 was prepared by treating of powdered Fe metal with HF at 180 ^{o}C for two weeks, AgF_2 was obtained by fluorination of $AgNO_3$ in liquid aHF. $M(SbF_6)_2$ (M = Ca, Mn, Fe, Ni, Cr, Ag, Cd, Sn) [16,17] and H_3OSbF_6 [18] were prepared as described previously. SbF_5 was prepared by fluorination of SbF_3 in a nickel autoclave at 200 ^{o}C for 24 h and distillated twice before use. Anhydrous HF (Fluka, Purum) was treated with K_2NiF_6 (Ozark Mahoning) for several hours prior to use.

4.2. Raman Spectroscopy

Raman spectra were recorded (10–20 scans) on a Renishaw Raman Imaging Microscope System 1000, with the 632.8 nm exciting line of a He-Ne laser (50 mW) with a resolution of 2 cm^{-1} and on Horiba Jobin-YvonLabRAM HR spectrometer using the 632.81 nm excitation line of He-Ne laser (17 mW). Some of the Raman spectra are given in Supplementary Material (**Figs. S4 and S5**).

4.3. Powder X–ray Diffraction Photographs

X-ray powder diffraction photographs (**Table S1**) were obtained using the Debye-Scherrer technique with Ni-filtered CuK_α radiation. Samples were loaded into quartz capillaries (0.3 mm) in a dry-box. Intensities were estimated visually.

4.4. Reactions between MO (M = Be, Mg, Ca, Sr, Ti, V, Nb, Mn, Ni, Cu, Zn, Pd, Hg, Sn, Pb) and SbF_5 in aHF

MO was loaded in a reaction vessel in a glove-box (**Table 2**). aHF and SbF_5 were condensed onto the reaction mixture and the reaction vessel was brought to room temperature. The reaction mixtures were left stirring at room temperature (**Table 2**). Volatiles were slowly pumped off at room temperature for few hours, leaving colourless (Be, Mg, Ca, Sr, Mn, Cu, Zn, Hg, Sn, Pb), yellow (Ni), black (Pd), greenish-yellow (V), greyish (Ti, Nb) solids (**Table 2**).

In the case of Pd additional experiment was done. Fluorine was added onto PdO/SbF_5/aHF reaction mixture resulting in a green solution from which green material was recovered (**Table 1**).

4.5. Attempted Reactions between MO (M = Ti, V, Nb) and liquid aHF

Around 100 mg of MO (M = Ti, V, Nb) was loaded in a reaction vessel in a glove-box. After 5-6 ml of aHF was condensed onto them, the reaction vessels were brought to room temperature. After one week of intesive stirring there was no visible change. Volatiles were pumped away and only starting MO were recovered.

4.6. Reactions between H_3OSbF_6 and $M(SbF_6)_2$ (M = Ca, Mn,Fe, Co Ni, Sn) and SbF_5 in aHF

Appropriate mixtures of H_3OSbF_6 and $M(SbF_6)_2$ (M = Ca, Mn, Fe, Co, Ni, Sn) were loaded in a reaction vessel in a glove-box and aHF and SbF_5 were condensed onto the reaction mixture and the reaction vessel was brought to room temperature (**Table 3**). Colourless (Ca, Mn, Fe, Sn), pink (Co), yellow (Ni), solutions were obtained. Volatiles were slowly pumped off at room temperature, leaving behind colourless (Ca, Mn, Fe, Sn), pink (Co) and yellow (Ni) solids (**Table 3**).

4.7. Crystal Growth

Crystal growth of the products obtained by reactions between MO (M = Mg, Ca, Ni, Cu, Zn, Sn) and SbF_5 in aHF (Table 2), crystal growth of the products obtained by reactions between H_3OSbF_6 and $M(SbF_6)_2$ (M= Ca, Mn, Fe, Co, Ni, Pd, Sn) in aHF (**Tables 2 and 3**) and direct crystal growth of H_3OSbF_6 / $M(SbF_6)_2$ (M = Cr, Ag, Cd) mixtures (**Table 3**) were carried out in a double T–shaped apparatus consisting of two FEP tubes (19 mm. o.d., and 6 mm. o.d.). Starting materials were loaded into the wider arm of the crystallization vessel in a dry-box. aHF (~4–8 ml) was then condensed onto the starting material at 77 K. The crystallization mixtures were brought up to ambient temperature and the clear solutions were decanted into the narrower arm. The evaporation of the solvent from these solutions was carried out by maintaining a temperature gradient corresponding to about 10 K between both tubes. The effect of this treatment was to enable aHF to be slowly evaporated from narrower into wider tube leaving the crystals. When the HF level in the narrower arm of crystallization vessel ceased to further decrease, it was necessary to increase the temperature gradient. This was accomplished by slowly cooling the larger arm in a cryostat from +12 °C to –30 °C and down to –55 °C to induce crystallization.

Single crystals of colourless $H_3OM(SbF_6)_3$ (M = Mg, Zn) and $(H_3O)_3M(SbF_6)_5$ (M = Mn, Cd), pink $H_3OCo(SbF_6)_3$ and green $(H_3O)_3Pd(SbF_6)_5$ were grown from solutions of corresponding starting compounds. All other attempts to prepare single crystals of $[H_3O]^+/M^{2+}/[SbF_6]^-$ compounds failed (**Tables 2 and 3**).

Crystallization of $H_3OSbF_6/Cr(SbF_6)_2$ proceeded in a similar way as reported for $XeF_5SbF_6/Cr(SbF_6)_2$ mixture. After addition of aHF onto $H_3OSbF_6/Cr(SbF_6)_2$ mixture, green precipitate formed immediately with a colorless clear liquid phase present above. The liquid phase with some undissolved green material was poured into the narrower arm of crystallization vessel. After 40 days a few yellow-orange crystals of $(H_3O)_3[Cr^{IV}(SbF_6)_6](Sb_2F_{11})\cdot HF$ were grown on the surface of the green insoluble material. Everything was covered with a sticky, very dense liquid phase, most likely a mixture of HF and SbF_5.

Crystallization products were immersed in perfluorinated oil (ABCR, FO5960, melting point 263 K) in a dry-box. Single crystals were then selected from the crystallization products under the microscope (at temperatures between 265 to 273 K) outside the dry-box and then transferred into the cold nitrogen stream of the diffractometer.

Selected single crystals were transferred to 0.3 mm quartz capillaries inside the dry box and their Raman spectra were recorded at several random positions (**Fig. S5**).

4.8. X-ray Structure Determinations

Single-crystal data of $(H_3O)M(SbF_6)_3$ (M = Co, Zn) were collected on a Rigaku AFC7 diffractometer equipped with a Mercury CCD area detector, using graphite monochromatized MoK_α radiation. Because of poor quality of $H_3OM[SbF_6]_3$ (M = Zn, Co) crystals only lattice parameters were determined.

Single-crystal data for $(H_3O)Mg(SbF_6)_3$, $(H_3O)_3M(SbF_6)_5$ (M = Mn, Pd, Cd) and $(H_3O)_3[Cr^{IV}(SbF_6)_6](Sb_2F_{11})\cdot HF$ were collected on a Gemini A diffractometer equipped with an Atlas CCD detector, using graphite monochromated Mo–Kα radiation. The data were treated using the CrysAlisPro software suite program package.[19] Analytical absorption corrections were applied to all the data sets. The structures were solved with the charge-flipping method using the Superflip program[20] (Olex crystallographic software[21]). The electron density map, obtained with Superflip software, was analyzed using the EDMA program[22], which gave initial models of the structures. Some structures were solved using the SHELXS program.[23] Structure refinement was performed with the SHELXL-2014[24] software, implemented in the program package WinGX.[25] The structure drawings were generated by DIAMOND 4.2.2 software.[26]

During the refinement of $(H_3O)_3[Cr^{IV}(SbF_6)_6](Sb_2F_{11})\cdot HF$, the twinning law -1 0 0 0 -1 0 0 0 1 was derived using TwinRotMat procedure implemented in the Platon software [27]. Its use resulted in a nearly 1:1 ratio of two different domains. Because of too large thermal parameters of Sb10 atom and because of the presence of noticeable peak of residual electron density near this atom, the Sb10 atom was split over two position, i.e. Sb10 and Sb11. The occupancy of ½ was set for both of them. Because of strongly elongated thermal ellipsoid for F94 atom, the position of the latter was also split, and the ratio between occupancies of F94a and F94b centres were refined giving at the final stage ratio 0.58:0.42.

Peaks of electron density found outside the coordination sphere of Sb or Cr atoms, were identified as O (H_3O) or F (HF) moieties. Because of rather poor quality of collected diffraction data the positions of hydrogen atoms weren't localized. Proposed distinction between O and F atoms (i.e. $[H_3O]^+$ cations and neutral HF molecules) was done on the basis of: a) occupancy refinement, b) analysis of the number and geometry of the closest $X\cdots F–SbF_5$ (X = O or F) contacts, c) assumption that the chromium oxidation state is +4 (see paragraph 2.1.) and d) charge balance requirements.

All hydrogen atoms in the crystal structure of $(H_3O)Mg(SbF_6)_3$ and some hydrogen atoms in the crystal structures of $(H_3O)_3Mn(SbF_6)_5$ and LT-$(H_3O)_3Pd(SbF_6)_5$ compounds were localized from the difference Fourier maps. Positions of the rest of hydrogen atoms in the latter two compounds, and all hydrogen atoms in structures of HT-$(H_3O)_3Pd(SbF_6)_5$ were placed on reported positions on the basis of geometrical reasons, i.e. taking into account the geometry of $[H_3O]^+$ cation and the orientation of closest $O\cdots F$ contacts. Before the final refinement isotropic thermal parameters of hydrogen atoms were set as 1.2 equivalent thermal parameter of respective oxygen atom and geometrical restrictions (DFIX) have been used.

The CIF's files can be obtained from Fachinformationszentrum Karlsruhe, 76344 Eggenstein-Leopoldshafen, Germany (e-mail: crysdata@fiz-karlsruhe.de; http://www.fiz-karlsruhe.de/request_for_deposited_data.html) on quoting the appropriate CSD number: CSD–432046 ($(H_3O)_3Mn(SbF_6)_5$), CSD–432047 (LT-$(H_3O)_3Pd(SbF_6)_5$), CSD– 432048 (HT-$(H_3O)_3Pd(SbF_6)_5$), CSD–432049 ($(H_3O)Mg(SbF_6)_3$) and CSD–432050 ($(H_3O)_3[Cr^{IV}(SbF_6)_6](Sb_2F_{11})\cdot HF$).

Acknowledgements

The authors (Z.M., E. G.) gratefully acknowledge the Slovenian Research Agency (ARRS) for the financial support of the present study within the research program: P1–0045 Inorganic Chemistry and Technology. They are also very grateful to Prof. Florian Kraus for measuring some X-ray powder diffraction patterns.

Appendix A. Supplementary data

Supplementary data associated with this article can be found, in the online version, at...

References

[1] Z. Mazej, E. Goreshnik, Z. Jagličić, Eur. J. Inorg. Chem. (2012) 1734–1741.

[2] Z. Mazej, E. Goreshnik, J. Fluorine Chem.130 (2009) 399–405.

[3] K. Lutar, B. Žemva, H. Borrmann, Eur. J. Solid State Inorg.Chem. 33 (1996) 957–969.

[4] Z. Mazej, G. Tavčar, Inorg. Chim. Acta 377 (2011) 69–76.

[5] T. A. O'Donnell, Superacids and Acidic Melts as Inorganic Chemical Reaction Media, VCH Publishers, New York, **1993**.

[6] Z. Mazej, E. Goreshnik, Eur. J. Inorg. Chem. (2016) 3356–3364.

[7] C.G. Barraclough, R.W. Cockman, T.A. O'Donnell, W.S.J. Schofield, Inorg. Chem. 21 (1982) 2519–2521.

[8] Z. Mazej, E. Goreshnik, J. Fluorine. Chem. (2016), in press, DOI: 10.1016/j.jfluchem.2016.05.014.

[9] Z. Mazej, E. Goreshnik, Z. Kristallogr. 230 (2015) 123–130.

[10] R. D. Shannon, Acta Crystallogr A 32 (1976) 751–767.

[11] P. Benkič, Z. Mazej, Z. anorg. allg. Chem. 627 (2001) 1952–1957.

[12] Z. Mazej, P. Benkič, A. Tressaud, B. Žemva, Eur. J. Inorg. Chem. (2004) 1827–1834.

[13] P. Benkič, Z. Mazej, B. Žemva, Angew. Chem. Int. Ed. 41 (2002) 1398–1399.

[14] Z. Mazej, E. Goreshnik, Eur. J. Inorg. Chem. 2008 (2008) 1795–1812.

[15] PTFE valves were constructed and made at Jožef Stefan Institute in a similar way as shown in: O'Donnelll, *The Chemistry of Fluorine; in Comprehensive Inorganic Chemistry*, Pergamon Press, Oxford, 1973, p. 1918.

[16] D. Gantar, I. Leban, B. Frlec, J.H. Holloway, J. Chem. Soc., Dalton Trans (1987) 2379–2383.

[17] Z. Mazej, J. Fluorine Chem. 125 (2004) 1723–1733.

[18] K.O. Christe, C.J. Schack, R.D. Wilson, Inorg. Chem. 14 (1975) 2224–2230.

[19] CrysAlisPro, Agilent Technologies, Version 1.171.37.31 (release 14-01-2014 CrysAlis171 .NET).

[20] L. Palatinus, G. Chapuis, J. Appl. Cryst. 40 (2007) 786–790.

[21] O.V. Dolomanov, L.J. Bourhis, R.J. Gildea, J.A.K. Howard, H. Puschmann, J. Appl. Cryst. 42 (2009) 339–341.

[22] L. Palatinus, S. Jagannatha Prathapa, S. van Smaalen J. Appl. Cryst. 45 (2012) 575

[23] G. M. Sheldrick, Acta Cryst. A64 (2008) 112–122.

[24] G.M. Sheldrick, Acta Cryst. C71 (2015) 3−8.

[25] L.J. Farrugia., J. App. Cryst. 45 (2012) 849–854.

[26] Diamond - Crystal and Molecular Structure Visualization Crystal Impact - Dr. H. Putz & Dr. K. Brandenburg GbR, Kreuzherrenstr. 102, 53227 Bonn, Germany http://www.crystalimpact.com/diamond

[27] A.L. Spek, Acta Cryst. D65 (2009) 148–155.

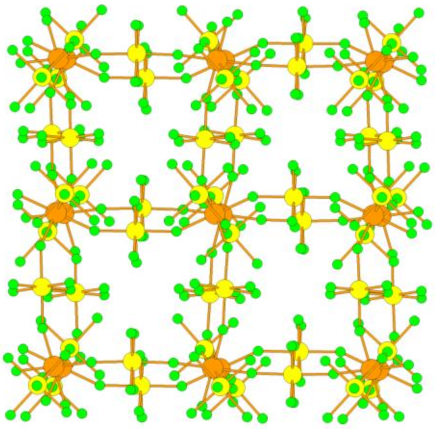

Fig. 1. Three-dimensional framework composed of M^{2+} cations interconnected by XF_6 octahedra in the crystal structures of $AM(XF_6)_3$ (A = $[O_2]^+$, $[NO]^+$, $[NH_4]^+$, K^+, Rb^+, Cs^+, $[XeF_5]^+$; M = divalent metal; X = As, Sb). Single charged cations are omitted for clarity.

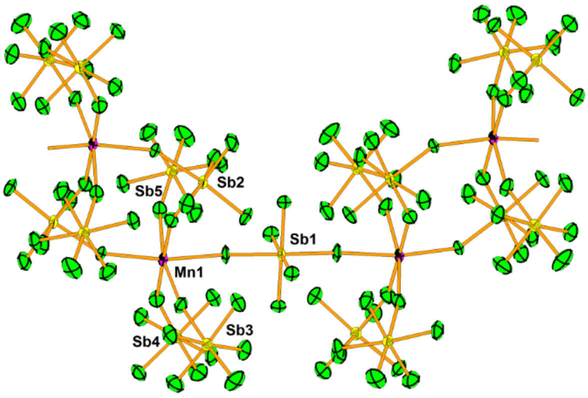

Fig. 2. Part of the $([Mn_2(SbF_6)_9]^{5-})_n$ column in the crystal structure of $(H_3O)_3Mn(SbF_6)_5$ (thermal ellipsoids are drawn at the 50% probability level).

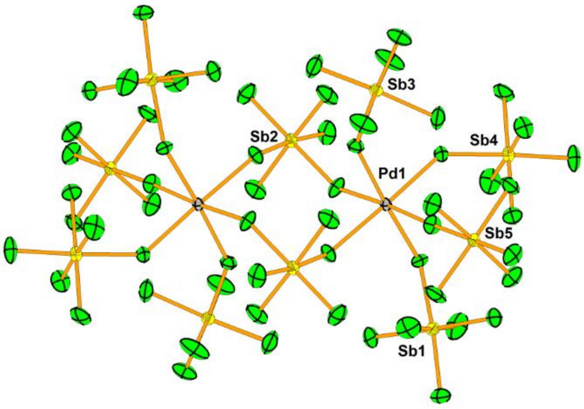

Fig. 3. The $[Pd(\eta^1\text{-}SbF_6)_4]$–$(cis\text{-}\eta^2\text{-}SbF_6)_2$–$[Pd(\eta^1\text{-}SbF_6)_4]$ moiety in the crystal structure of β-modification of $(H_3O)_3Pd(SbF_6)_5$ (thermal ellipsoids are drawn at the 50% probability level).

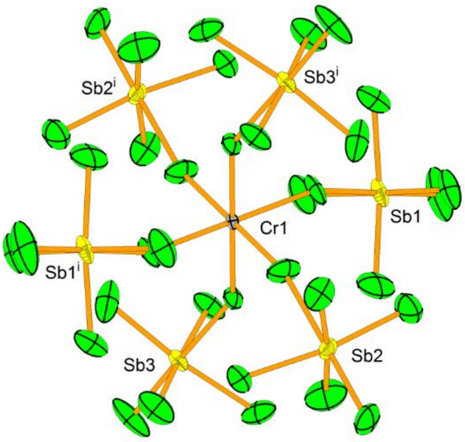

Fig. 4. Part of the crystal structure of $(H_3O)_3[Cr^{IV}(SbF_6)_6](Sb_2F_{11})\cdot HF$ showing discrete $[Cr(SbF_6)_6]^{2-}$ group (thermal ellipsoids are drawn at the 50% probability level).

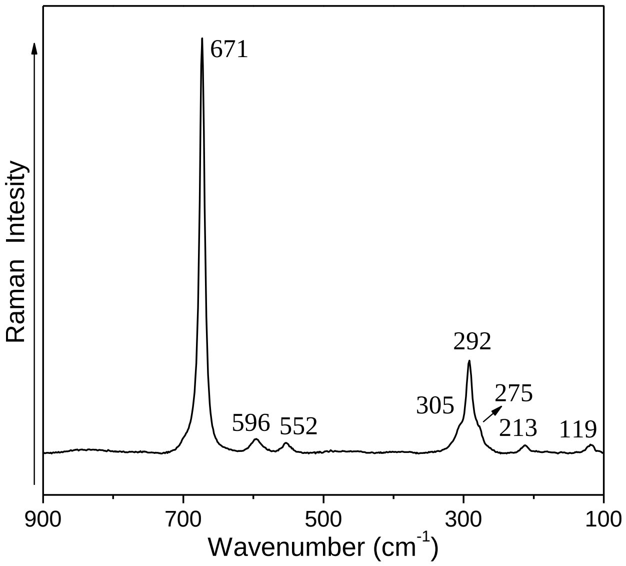

Fig. 5. Raman spectrum of $H_3OMg(SbF_6)_3$.

Table 1

Summary of crystal data and refinement results for $H_3OMg(AsF_6)_3$, $(H_3O)_3M(SbF_6)_5$ (M = Mn, Pd) and $(H_3O)_3[Cr^{IV}(SbF_6)_6](Sb_2F_{11})\cdot HF$.[a]

Formula	$H_3OMg(SbF_6)_3$	$(H_3O)_3Mn(SbF_6)_5$	LT-$(H_3O)_3Pd(SbF_6)_5$	HT-$(H_3O)_3Pd(SbF_6)_5$	$(H_3O)_3[Cr^{IV}(SbF_6)_6](Sb_2F_{11})\cdot HF$
Fw	750.58	1290.76	1342.27	1342.27	1995.70
T (K)	200	200	200	293	150
Crystal system	orthorhombic	monoclinic	triclinic	monoclinic	monoclinic
Space group	$Pnma$	$P2_1/m$	$P\bar{1}$	$C\,2/c$	$P\,2_1/m$
a (Å)	10.6330(7)	10.5743(3)	10.7217(2)	15.3036(3)	9.9725(2)
b (Å)	14.6887(11)	21.7430(5)	10.7563(2)	15.3901(3)	22.4411(6)
c (Å)	9.60007(7)	10.8011(3)	22.7684(5)	22.7805(5)	17.6694(4)
α (deg)	90	90	102.766(2)	90	90
β (deg)	90	91.463(2)	102.673(2)	108.188(2)	90.035(2)
γ (deg)	90	90	90.538(2)	90	90
V (Å^3)	1499.49(19)	2482.55(11)	2493.86(9)	5097.29(18)	3954.29(17)
Z	4	4	4	8	4
λ (Å)	0.71069	0.71069	0.71069	0.71069	0.71069
μ (mm^{-1})	5.598	6.085	6.273	6.138	5.872
D_{calcd} (g/cm^3)	3.325	3.453	3.575	3.511	3.296
R_1[b]	0.0446	0.035	0.0405	0.024	0.046
wR_2[c]	0.1082	0.0727	0.0904	0.055	0.1240
GOF indicator[d]	1.298	1.058	1.417	1.058	1.072

[a] Unit cells of $H_3OM(SbF_6)_3$ (M = Zn, orthorhombic at 200 K: 10.6775 Å, 14.6424 Å, 9.5462 Å; M = Co, orthorhombic at 200 K: 10.8360Å, 14.4746Å, 9.6268 Å) and $(H_3O)_3Cd(SbF_6)_5$ (tetragonal at 200 K: 10.797(14) Å, 10.797(14) Å, 43.25(3) Å).[b] $R_1 = \Sigma||F_o| - |F_c|\Sigma/||F_o|$ for $I > 2\sigma(I)$. [c] $wR_2 = [\Sigma[w(F_o^2 - F_c^2)^2]/\Sigma(w(F_o^2)^2]^{1/2}$. [d] $GOF = [\Sigma w(F_o^2 - F_c^2)^2/(N_o - N_p)]^{1/2}$, where N_o = no. of reflns and N_p = no. of refined parameters.

Table 2

Experimental conditions for the reactions between MO (Be, Mg, Ca, Sr, Ti, V, Nb, Mn, Ni, Cu, Zn, Pd, Hg, Sn, Pb) and SbF$_5$ in aHF and observed reaction and crystallization products.

	Starting compounds				V aHF / ml	Time of reaction / d	Observed products after reaction	Time of crystallization / d	bserved single crystals pon the crystallization f reaction products
	MO / mg	MO / mmol	SbF$_5$ / mg	SbF$_5$ / mmol					
BeO	20	0.8	650	3.00	4	3[a]	BeO	/[b]	/
MgO	42	1.04	1000	4.61	4	1[c]	$H_3OMg(SbF_6)_3$	70	$H_3OMg(SbF_6)_3$
CaO	47	0.83	700	3.23	4	1[c]	$Ca(SbF_6)_2/H_3OSbF_6$	28	$H_3OSbF_6/H_3OSb_2F_{11}$
SrO	123	1.18	1000	3.00	3	1[c]	$Sr(SbF_6)_2/H_3OSbF_6$	/[b]	/
TiO	32	0.5	480	2.2	3	20[d]	$H_3OSbF_6/TiF_3/TiF_4$	/[b]	/
VO	38	0.57	480	2.2	4	24[d]	$H_3OSb_2F_{11}/VF_3$	/[b]	/
NbO	60	0.55	550	2.52	4	24[d]	$H_3OSbF_6/H_3OSb_2F_{11}/H_3ONbF_6$	/[b]	/
MnO	97	1.37	1400	6.46	4	8[c]	$Mn(SbF_6)_2/H_3OSb_2F_{11}$	/[b]	/
NiO	102	1.36	500	3.69	4	5[c]	$H_3ONi(SbF_6)_3$	/[b]	/
NiO	72	0.96	1000	4.61	3	3[c]	$H_3ONi(SbF_6)_3$	19	yellow powder
CuO	82	1.03	900	4.15	4	1[c]	$H_3OCu(SbF_6)_3$	20	stacked plates
ZnO	89	1.09	1000	4.61	4	1[c]	$H_3OZn(SbF_6)_3$	21	$H_3OZn(SbF_6)_3$
PdO	85	0.7	600	2.77	4	3[a]	PdO	/[b]	/
PdO	85	0.7	600	2.77	4	1[e]	$Pd(SbF_6)_2/H_3OSbF_6$	19	$(H_3O)_3Pd(SbF_6)_5/H_3OSbF_6/Pd(SbF_6)_2$
HgO	99	0.46	1100	5.07	3	1[c]	$Hg(SbF_6)_2/H_3OSbF_6$	/[b]	/
SnO	90	0.67	800	3.69	4	1[c]	$Sn(SbF_6)_2/H_3OSb_2F_{11}$	67	white powder
PbO	103	0.46	1400	6.46	3	1[c]	$Pb(SbF_6)_2/H_3OSb_2F_{11}$	/[b]	/

[a] Undissolved. [b] Crystallization wasn't attempted. [c] Clear solution. [d] Partly dissolved. [e] After addition of F_2 clear green solution formed.

Table 3
Experimental conditions for the reactions between H_3OSbF_6 and $M(SbF_6)_2$, (M = Ca, Cr, Mn, Fe, Co Ni, Ag, Cd, Sn) and observed reaction and crystallization products

	Starting compounds				V aHF	Time of reaction	Observed products	Time of ystallization	bserved single crystals upon the crystallization
	$M(SbF_6)_2$		H_3OSbF_6						
	/ mg	/ mmol	/ mg	/ mmol	/ ml	/ d	after reaction	/ d	of reaction products
$Ca(SbF_6)_2$	247	0.48	128	0.50	3	2[a]	$Ca(SbF_6)_2/H_3OSbF_6$	68	$H_3OSbF_6/H_3OSb_2F_{11}$
$Mn(SbF_6)_2$	263	0.5	127	0.50	3[b]	3[a]	$Mn(SbF_6)_2/H_3OSb_2F_{11}$	35	$(H_3O)_3Mn(SbF_6)_5$
$Mn(SbF_6)_2$	263	0.5	255	1.00	3	3[a]	$Mn(SbF_6)_2/H_3OSbF_6$	55	$(H_3O)_3Mn(SbF_6)_5$
$Mn(SbF_6)_2$	263	0.5	383	1.50	3	3[a]	$Mn(SbF_6)_2/H_3OSbF_6$	35	$(H_3O)_3Mn(SbF_6)_5$ / H_3OSbF_6
$Fe(SbF_6)_2$	393	0.74	194	0.76	3	1[c]	$H_3OFe(SbF_6)_3$	34	stacked plates
$Co(SbF_6)_2$	464	8.88	223	0.88	2	9[a]	$H_3OCo(SbF_6)_3$	30	$H_3OCo(SbF_6)_3$
$Ni(SbF_6)_2$	554	1.05	261	1.03	2	1[a]	$H_3ONi(SbF_6)_3$	19	yellow powder
$Cr(SbF_6)_2$	85	0.16	40	0.16	5	/	/	40[d,e]	$(H_3O)_3[Cr^{IV}(SbF_6)_6](Sb_2F_{11})\cdot HF$
$Ag(SbF_6)_2$	105	0.18	46	0.18	5	/	/	24[e]	$Ag_3(SbF_6)_4/H_3OSbF_6$
$Cd(SbF_6)_2$	88	0.15	115	0.45	5	/	/	30[e]	$(H_3O)_3Cd(SbF_6)_5/H_3OSbF_6$
$Sn(SbF_6)_2$	533	0.90	230	0.90	2	4[c]	$Sn(SbF_6)_2/H_3OSbF_6$	19	white powder

[a] Clear solution. [b] 200 mg of SbF_5 was added. [c] Partly dissolved. [d] Clear colourless solution above green solid. [e] Direct crystallization without prior isolation and characterization of reaction products.